water

MDPI

Article

Hydrochemical Characteristics, Water Quality, and Evolution of Groundwater in Northeast China

Tao Zhang [1,2,†], Pei Wang [3,†], Jin He [1], Dandan Liu [1], Min Wang [4], Mingguo Wang [1,*] and Shibin Xia [2,*]

[1] Center for Hydrogeology and Environmental Geology, China Geological Survey, Baoding 071051, China; zhangtao1@mail.cgs.gov.cn (T.Z.); hejin@mail.cgs.gov.cn (J.H.); liudandan@mail.cgs.gov.cn (D.L.)
[2] School of Resources and Environmental Engineering, Wuhan University of Technology, Wuhan 430070, China
[3] State Key Laboratory of Freshwater Ecology and Biotechnology, Institute of Hydrobiology, Chinese Academy of Sciences, Wuhan 430072, China; pwang@ihb.ac.cn
[4] Zhoukou Vocational and Technical College, Zhengzhou 466000, China; wangmin2060@163.com
* Correspondence: wangmingguo@mail.cgs.gov.cn (M.W.); xiashibin@126.com (S.X.); Tel.: +86-153-928-80268 (S.X.)
† These authors contributed equally to this work.

Abstract: Groundwater is vital to local human life and agricultural irrigation, and the quality of the water is critical to human health. As a result, it is critical to investigate the hydrochemical evolution and water quality of groundwater in the Sanjiang Plain. There were 259 samples obtained. Furthermore, hydrogeochemical simulation was performed to highlight groundwater's hydrochemical features, evolution process, and water quality. The analytical results show that the groundwater in the study area is somewhat alkaline with a mean TDS of 285.94 mgL^{-1} and the primary contributing ions being Ca^{2+} and $HCO_3{}^-$. The closer the concentration of TDS and $NO_3{}^-$ is to the city, the higher the concentration, indicating that the chemical composition of the water body has been affected by certain human activities. The Piper diagram, Gibbs diagram, and correlation analysis results demonstrate that the chemical type of groundwater is mostly HCO_3-Ca and the hydrochemistry is primarily regulated by weathering and carbonate and silicate dissolution. According to the entropy-weighted water quality index, the groundwater quality in this location is pretty acceptable. This study could help strengthen groundwater quality monitoring based on local conditions, identify the source of nitrate, provide data support for the safe use of local water resources, and serve as a reference for global water chemical evolution and water quality evaluation in cold regions.

Keywords: groundwater; hydrochemistry; water quality; WQI; Sanjiang Plain

Citation: Zhang, T.; Wang, P.; He, J.; Liu, D.; Wang, M.; Wang, M.; Xia, S. Hydrochemical Characteristics, Water Quality, and Evolution of Groundwater in Northeast China. *Water* **2023**, *15*, 2669. https://doi.org/10.3390/w15142669

Academic Editors: Christos S. Akratos, Guilin Han and Xiaolong Liu

Received: 13 June 2023
Revised: 4 July 2023
Accepted: 5 July 2023
Published: 24 July 2023

1. Introduction

Water is essential for the survival and growth of both animals and plants, and it also serves as the foundation for industrial and agricultural development. Water safety is critical to human existence [1–4]. Groundwater is frequently employed in industrial and agricultural production because of its steady water supply and generally acceptable water quality [4–8]. Groundwater has traditionally been used as a primary source of water, particularly in locations where rivers and lakes are underdeveloped [9–11]. Understanding the variance trend in regional groundwater quality and the variables that influence it is critical for fully using and rationally maintaining groundwater resources, avoiding and managing groundwater contamination, protecting people's health, and fostering economic growth. As a result, the researchers performed extensive study on groundwater contamination [12,13], focusing on three-nitrogen pollution and heavy metal pollution [14–16]. Pollutant movement, transformation, source, and health risk assessment were researched using statistical analysis, ion ratio, isotope analysis, and entropy weight analysis, yielding numerous findings [17–19].

Nitrate contamination is one of the most serious environmental geological issues that has to be addressed immediately [18,20]. Groundwater nitrate-nitrogen pollution

tends to be severe when urbanization speeds up and human activities intensify. NO_3-N is frequently used to assess the toxicity and eutrophication of water [21,22], and its high concentration will result in degradation of water quality, ecological damage, and a hazard to human health. NO_3-N undergoes a sequence of modifications that result in the formation of carcinogenic and teratogenic chemicals. Long-term use of nitrate-rich water raises the chance of people developing disorders such as methemoglobin. Furthermore, high nitrate levels have a negative impact on the biological environment, causing eutrophication and algal bloom. As a result, removing nitrate from groundwater has become a research priority.

Sanjiang Plain has an abundance of black land, which is ideal for cultivating food crops. Groundwater is frequently utilized to irrigate crops in this region [23,24]. The exploitation of groundwater is expanding as urbanization and industrialization progress, and human activities have an increasing influence on groundwater quality. There are many dry and paddy fields in the region, and groundwater is mostly utilized to irrigate crops. The hydrochemical composition of groundwater is continually changing as a result of overexploitation of groundwater, fertilization, irrigation, and other agricultural operations, and the deterioration of water quality will impair the safety of local agricultural and household water [25–27].

So far, the primary groundwater study paths in Sanjiang Plain have been a groundwater pollution risk model [28], shallow groundwater quality [29], and water resource allocation [30], with assessment research on the combination of groundwater pollution being very rare. The regional variable features and sources of major ions, as well as the overall water quality and control factors in the research area, need to be investigated further. As a result, this work focuses on the source and chemical evolution of groundwater in the Sanjiang Plain, and it investigates groundwater hydrochemistry using hydrochemical theory, multivariate statistical techniques, and a water quality index. In order to explain the mechanism of groundwater hydrochemistry evolution, the following three contents are largely investigated: (1) spatial distribution characteristics of groundwater chemistry, (2) groundwater hydrochemical evolution, and (3) groundwater quality. It is expected to provide a hydrochemical foundation for better revealing the variation trend of groundwater quality and environmental factors, as well as realizing the Sanjiang Plain groundwater management objectives of food security, ecological security, and water supply security. This work will serve as a resource for assessing water chemical evolution in frigid places across the world.

2. Materials and Methods

2.1. Study Area

The Sanjiang Plain is situated in the Heilongjiang Province, China (Figure 1). The Sanjiang Plain's mountains rose and the plain sank as a result of tectonic and neotectonic activity, and quaternary strata 100–300 m thick were deposited in the lower plain region. The principal river that flows through the study region is the Naoli River, which is a tributary of the Wusuli River. It rises in the Nadanhada Mountains of the Wanda Mountains, between Qitaihe and Mishan in the Heilongjiang Province, and runs through Qitaihe, Baoqing, Fujin, and Raohe before joining the Wusuli River in Dong'an Town. The overall length is 596 km, the main river channel is 20–100 m wide, the curvature coefficient is 1.4–3.0, and the gradient of the river channel is 1/2000–1/8000. There are nine rivers that flow into the upper reaches, eleven rivers that flow into the middle and lower sections, and a total of twenty tributaries in the basin. The river channels are meandering and serpentine, with crisscrossing river branches. Both sides were previously highly forested, with plentiful plankton growth and great fishing productivity conditions. This area's climate belongs to the temperate zone's humid and semi-humid continental monsoon climatic zone, which is marked by rapid spring warming, frequent wind and little rain, and the occurrence of spring drought. Summer is warm and humid, with frequent rainstorms and flash floods. The sky is high and the air is cool in fall; the temperature drops swiftly, and frost and cold waves arrive early. Winter is cold and dry, with ice and snow, although it is mainly bright.

The annual average temperature is 3.5 °C, with July being the warmest month and the monthly average temperature being 21.9 °C; January is the coldest month, with a monthly average temperature of −18.1 °C, an annual sunshine duration of approximately 2500 h, a frost-free period of approximately 140 days, and a maximum depth of 2.2 m. The yearly precipitation average is 537.2 mm. The yearly evaporation rate is 670.8 mm.

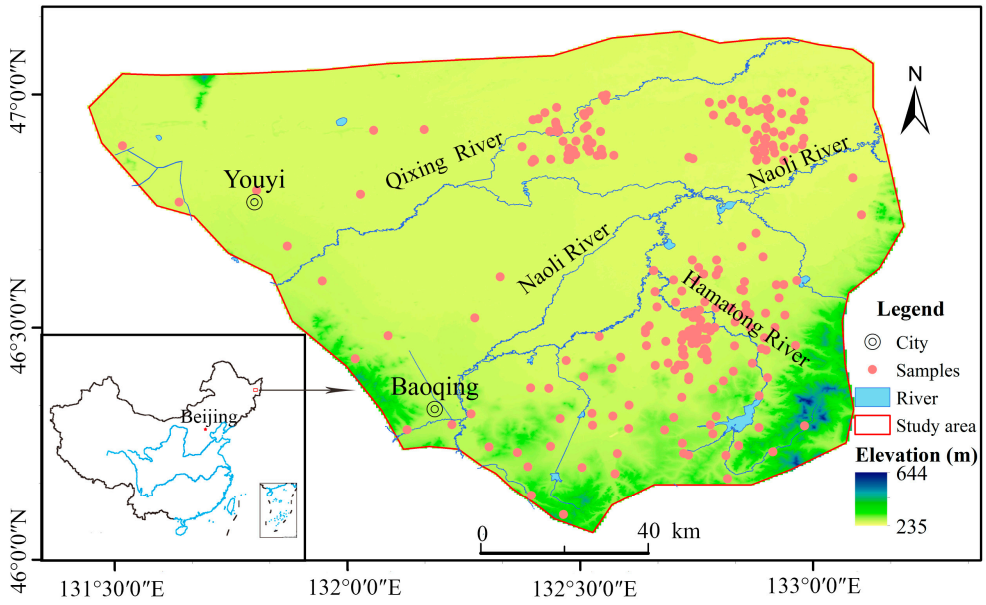

Figure 1. Spatial distribution of groundwater samples.

The regional aquifer system is divided into three compartments based on topography, landform, hydrology, and aquifer geological structure: the Quaternary pore aquifer system, the Paleogene–Neogene pore fissure aquifer system, and the Quaternary bedrock fissure aquifer system. The aquifer formations from bottom to top are the Lower Pleistocene Suibin Formation, the Middle Pleistocene Nongjiang Formation, the Upper Pleistocene Xiangyangchuan Formation, and the Biela Formation, according to the lithology, origin, and distribution of the Quaternary pore aquifer system. The sediments of different ages and sources in the alluvium and strata of the Honghe River are overlying structures between aquifers. There is no obvious water barrier in the middle, and the weak permeable layer is discontinuous, which is a uniform and large-thickness aquifer. The quaternary pore water may be separated into three strata based on groundwater circulation depth and runoff intensity: shallow, medium, and deep. Extracted from the Heilongjiang River, groundwater in the region flows generally from the southwest to the northeast. The major source of groundwater recharge is atmospheric precipitation, followed by lateral runoff replenishment of rivers, recharge of river water during flood times, and infiltration of swamp water. The main excretion routes are runoff, evaporation, and artificial mining.

Sanjiang Plain features flat topography, abundant land resources, little pollution, and significant agricultural development potential. This area has a relative scarcity of water resources, which are mostly used to irrigate crops by pumping groundwater. Since the end of the twentieth century, agricultural activities have increased, particularly the planting of well-irrigated rice. Groundwater alone cannot cover the water requirements of agricultural irrigation due to its scarcity. As a result, a huge number of tube wells have been developed and groundwater extraction has expanded fast, resulting in various ecological concerns such as wetland degradation, a major reduction in grassland area compared to previous periods, the loss of pump wells, and a reduction in rice output. The issue of groundwater quality is also fairly prevalent in this area. Trace indicators such as NH_4^+, NO_3^-, NO_2^-, COD_{Mn}, Fe^{2+}, and Mn^{2+} exceed the limit at a very high rate, which is the primary source of groundwater quality degradation.

2.2. Sample Collection and Analysis

A total of 259 groundwater samples were taken (Figure 1). The water sample was filtered and placed in two plastic bottles. Nitric acid was added to one bottle of sample to make the pH of water sample 2 for the cation test, and another bottle was added to make the pH of water sample 2 for the other index test. The cation was measured using a flame atomic absorption spectrometer (ContrAA300, Thuringia, Germany) [31]. Cl^-, NO_3^-, and SO_4^{2-} were quantified using ion chromatographs (883i, Herisau, Swiss) [32]. Titration with hydrochloric acid was used to determine HCO_3^- and CO_3^{2-} [29]. Titration with disodium (EDTA) was used to calculate total hardness (TH) [32]. Total dissolved solids (TDSs) were measured using a weighing technique [32]. pH was measured in the field by the glass electrode method [32]. The relative standard deviation of all test indices was less than 5%.

2.3. Entropy-Weighted Water Quality Index (EWQI)

The entropy technique is an objective weighing approach that determines an index's dispersion degree by computing the entropy value [33–35]. The entropy technique was used to calculate the weights of hydrochemical indicators such as Na^+, Cl^-, SO_4^{2-}, NO_3^-, TDS, TH, and pH, and groundwater quality was assessed using the groundwater quality standard: excellent (WQI < 25), acceptable (25 < WQI < 50), medium (50 < WQI < 100), poor (100 < WQI < 150), or severely bad (WQI > 150) [36]. Before computing the overall score using these indications, because the influence on groundwater chemistry varies depending on the content of the test indicators, various data were translated to the same measurement standard to remove the inaccuracy caused by variable content. The entropy weight method's quality index evaluation value (EWQI) is the product of w_i and C_j is the concentration of j in groundwater, and S_j is the standard value of j in groundwater, and was calculated as Equation (1) [37]:

$$EWQI = \sum_{j=1}^{m} w_i \times \frac{C_j}{S_j} \quad (1)$$

3. Results and Discussion

3.1. Hydrochemical Composition and Hydrochemical Types

3.1.1. Chemical Composition Characteristics of Groundwater

The primary cations in groundwater are Ca^{2+} and Na^+. The concentration of groundwater ions shows the relationship $Ca^{2+} > Na^+ > Mg^{2+} > K^+$, with Ca^{2+} and Na^+ content ranges of 0.34–142.28 $mg \cdot L^{-1}$ and 2.75–65.22 $mg \cdot L^{-1}$, respectively, with mean values of 45.76 $mg \cdot L^{-1}$ and 23.23 $mg \cdot L^{-1}$ (Table 1).

Table 1. Statistics of major parameters in groundwater.

Chemical Parameter	Mean	Standard Deviation	Min	Max	NSPRC (NSPRC, 2017)	Coefficient Variation
$K^+/mg \cdot L^{-1}$	3.01	4.83	0.08	61.17	—	1.61
$Na^+/mg \cdot L^{-1}$	23.23	12.53	2.75	65.22	200.00	0.54
$Ca^{2+}/mg \cdot L^{-1}$	45.76	25.59	0.34	142.28	—	0.56
$Mg^{2+}/mg \cdot L^{-1}$	16.13	10.74	2.52	67.47	—	0.67
$Cl^-/mg \cdot L^{-1}$	12.45	15.31	1.77	109.02	250.00	1.23
$SO_4^{2-}/mg \cdot L^{-1}$	9.31	32.04	0.00	450.00	250.00	0.54
$HCO_3^-/mg \cdot L^{-1}$	255.28	138.65	0.00	682.63	—	3.16
$NO_3^-/mg \cdot L^{-1}$	10.21	24.57	0.00	205.00	88.60	2.41
$TDS/mg \cdot L^{-1}$	285.94	118.59	85.24	839.64	1000.00	0.41
$TH/mg \cdot L^{-1}$	178.33	93.62	20.80	474.95	450.00	0.52
pH	7.15	0.42	5.46	9.04	6.5–8.5	0.06

The anion is mostly HCO_3^-, and groundwater concentrations show a relationship of $HCO_3^- > Cl^- > SO_4^{2-} > NO_3^-$. The concentration ranges for HCO_3^- and NO_3^- were 0–682.63 mg·L^{-1} and 0–205.0 mg·L^{-1}, respectively, with mean values of 255.27 mg·L^{-1} and 10.21 mg·L^{-1}. In general, the greater the content, the closer to the metropolitan area. This is linked to the aggregation of urban populations, demonstrating that NO_3^- is heavily influenced by human activity.

The pH value, as an essential parameter, can represent information about hydrogeochemical equilibrium. The pH ranges from 5.46 to 9.04, with a mean value of 7.15, showing that the regional diversity of pH values is limited and that the groundwater samples are generally slightly alkaline. TDS and TH concentration variation ranges were 85.24–839.64 mg·L^{-1} and 20.80–474.95 mg·L^{-1}, respectively, with mean values of 285.94 mg·L^{-1} and 178.33 mg·L^{-1}, and the coefficients of variation were 41.47% and 52.50%, showing that the regional disparities in TDS and TH concentrations were considerable. TDS was found to be higher in the north–south direction and lower in the east–west direction. The greater the TDS of densely inhabited populations, the closer they were to towns, indicating that the high TDS of certain water samples was induced by human activity (Figure 2).

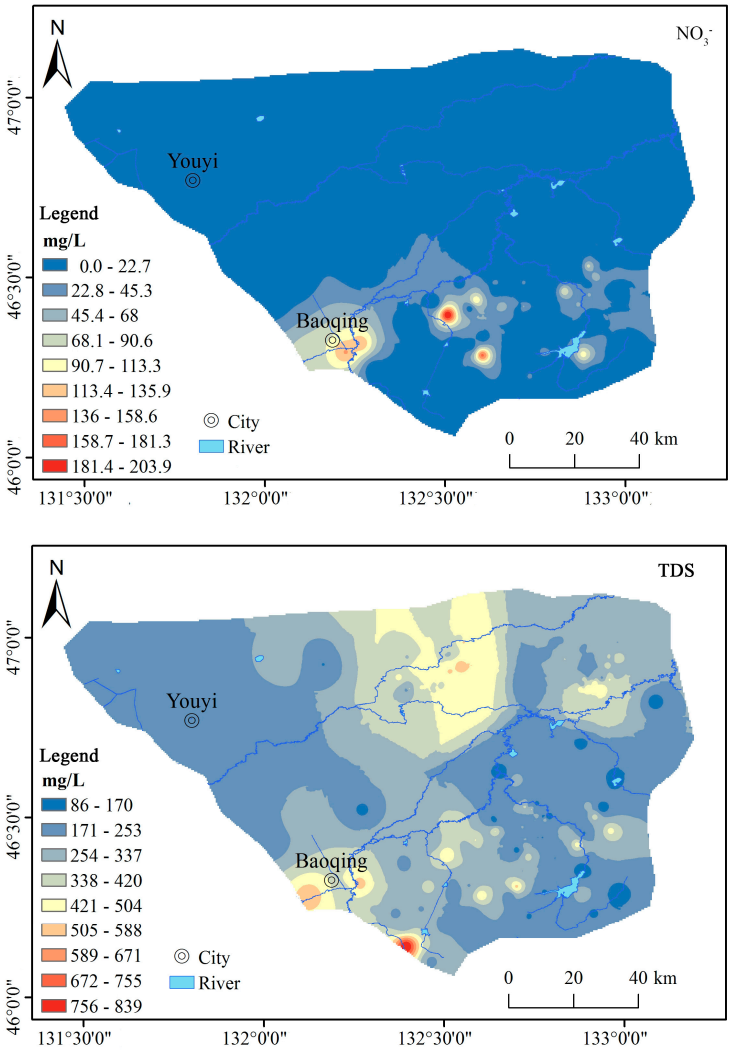

Figure 2. Distribution characteristics of NO_3^- and TDS.

3.1.2. Hydrochemical Type

The hydrochemistry and hydrochemical types were evaluated using a piper triplot, and the majority of the water samples fell towards Ca^{2+}, showing that Ca^{2+} is prevalent in

groundwater, followed by Mg^{2+}. All of the water sample points are near the HCO_3^- end of the anion diagram, indicating that HCO_3^- ions are common and that the chemical types are mostly HCO_3-Ca·Mg (Figure 3a). Ca^{2+} and HCO_3^-, on the other hand, are primarily derived from the dissolution of carbonate or silicate, indicating that this area is primarily governed by weathering and rock dissolution.

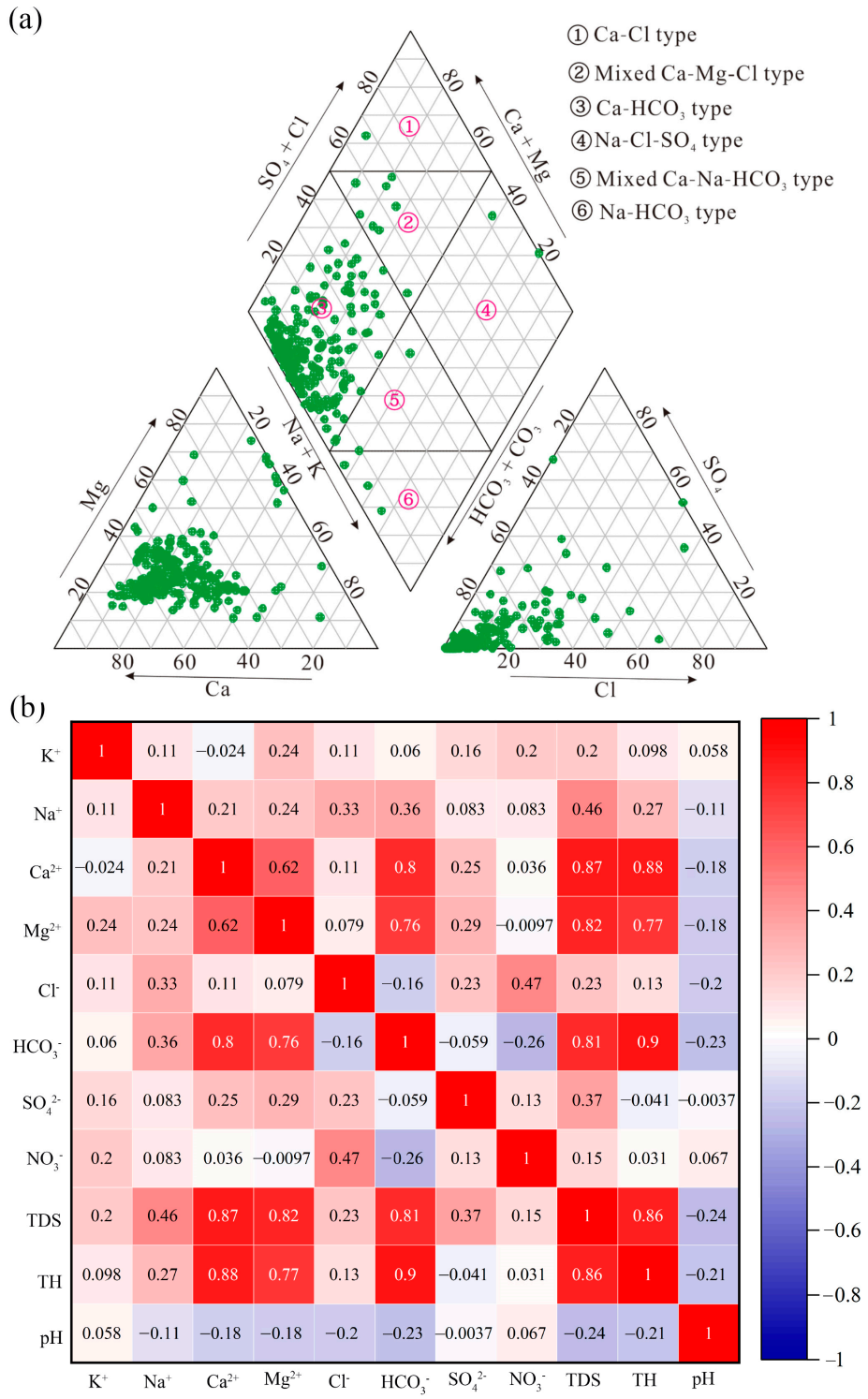

Figure 3. The piper plot of groundwater (**a**) and correlation between chemical parameters in groundwater of Sanjiang Plain (**b**).

3.1.3. Relationship between Chemical Indexes

Correlation analysis is frequently used to investigate the origin of ions in the evolution of hydrochemistry [24]. There is a strong link between the components of the same source. TDS has a high association with Na^+, Ca^{2+}, Mg^{2+}, SO_4^{2-}, and HCO_3^- (Figure 3b), indicating that Na^+, Ca^{2+}, Mg^{2+}, SO_4^{2-}, and HCO_3^- are the primary sources of groundwater TDS, among which TDS has a substantial correlation with Ca^{2+} ($R^2 = 0.866$, $p < 0.01$) and HCO_3^- ($R^2 = 0.813$, $p < 0.01$). The correlation coefficients between SO_4^{2-} and Ca^{2+}, Mg^{2+} are 0.251 and 0.288, respectively, showing that they have a similar material source, namely weathering dissolution and sulfuric acid dissolution of calcite, dolomite, and other carbonate minerals.

3.2. Control Factors of Groundwater Hydrochemistry

3.2.1. Natural Factors

The Gibbs model is commonly used to determine the primary water regulating parameters [38–42]. It consists of three governing endmembers: precipitation, rock weathering, and evaporative [43–45]. The atmospheric precipitation control area has a lower total dissolved solid concentration and a greater ratio of $Na^+/(Na^+ + Ca^{2+})$ and $Cl^-/(Cl^- + HCO_3^-)$, both of which are normally in the 0.5–1 range, and is dispersed in the bottom right corner of the Gibbs plot. The rock weathering area is in the middle left, the TDS value ranges from 70 to 300 $mg \cdot L^{-1}$, and the ratio is less than 0.5. The upper right of the diagram shows the evaporative crystallization control region, which has a greater TDS and a higher ratio (0.5–1). The TDS and ratios of the groundwater samples in this location are lower, and all samples fall within the rock weathering control area, indicating that the major ions in groundwater are caused by rock weathering (Figure 4a,b).

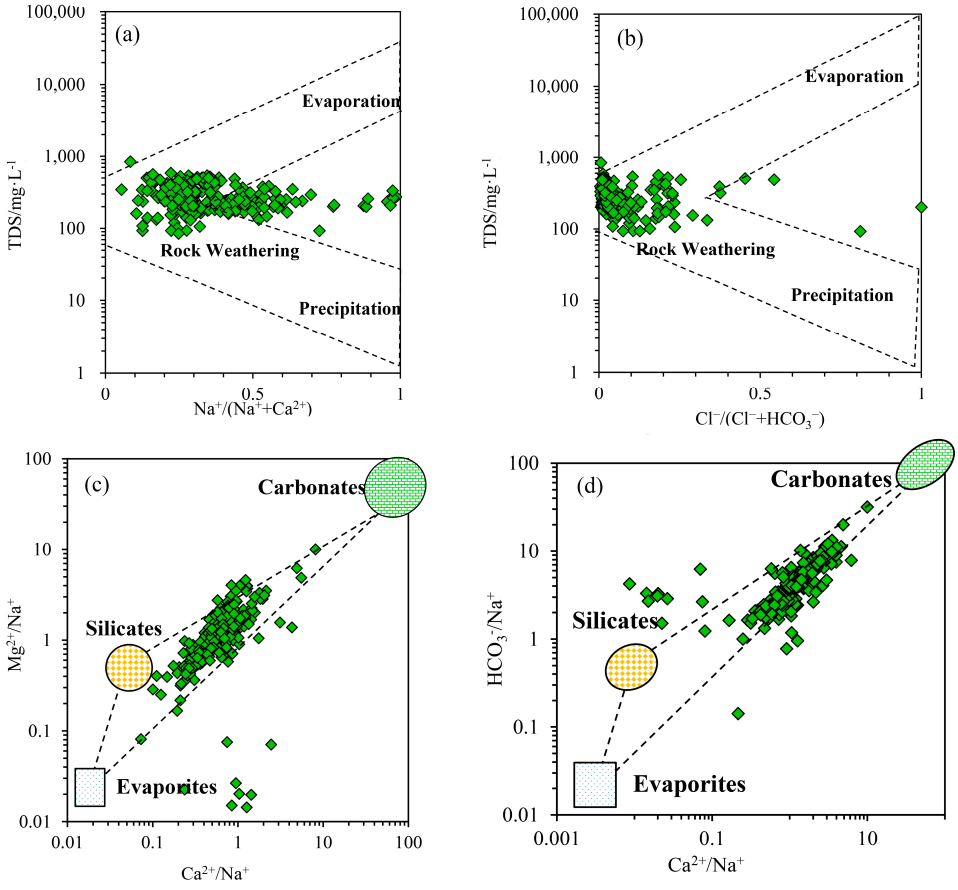

Figure 4. Gibbs plots of the groundwater samples (**a**,**b**) and plots of the relationship between HCO_3^-, Na^+, Ca^{2+}, and Mg^{2+} (**c**,**d**).

Various rocks will create different ions as they weather. The weathering of carbonate rock, silicate rock, and evaporite produces Ca^{2+} and Mg^{2+} in abundance. The main elements Na^+ and K^+ are formed through the weathering and disintegration of silicate rock and evaporite. Weathering and dissolution of carbonate and silicate rocks produce HCO_3^- in significant amounts. As a result of the breakdown of evaporated, SO_4^{2-} and Cl^- significant compounds are formed [46,47]. A mixing map generally reveals the source of ions created by chemical weathering in the watershed. Because the Ca^{2+}/Na^+, Mg^{2+}/Na^+, HCO_3^-/Na^+ relationships are unaffected by flow rate, dilution, or evaporation, they can reveal the hydrochemical origin and dissolution of minerals from which the major ions originate. The samples are located in the silicate rock and carbonate areas, demonstrating that groundwater is influenced by water–rock interaction (Figure 4c,d).

Cation alternating adsorption occurs when particles adsorb some cations in water and transform some of their initially adsorbed cations into water components under particular circumstances [48]. $(Na^+ - Cl^-)$ and $[(2SO_4^{2-} + HCO_3^-) - 2(Ca^{2+} + Mg^{2+})]$ $(mmol \cdot L^{-1})$ concentrations can be used to determine if $Na^+ - Ca^{2+}$ exchange occurs. The ratio $(Na^+ - Cl^-)/[(2SO_4^{2-} + HCO_3^-) - 2(Ca^{2+} + Mg^{2+})]$ should be close to 1:1 if the hydrogeochemical process is mostly cation exchange [49]. Water sample molar concentration ratios $(Na^+ - Cl^-)/[(2SO_4^{2-} + HCO_3^-) - 2(Ca^{2+} + Mg^{2+})]$ are typically near the 1:1 line, indicating that cation exchange is important in the subsurface hydrogeochemical process (Figure 5a).

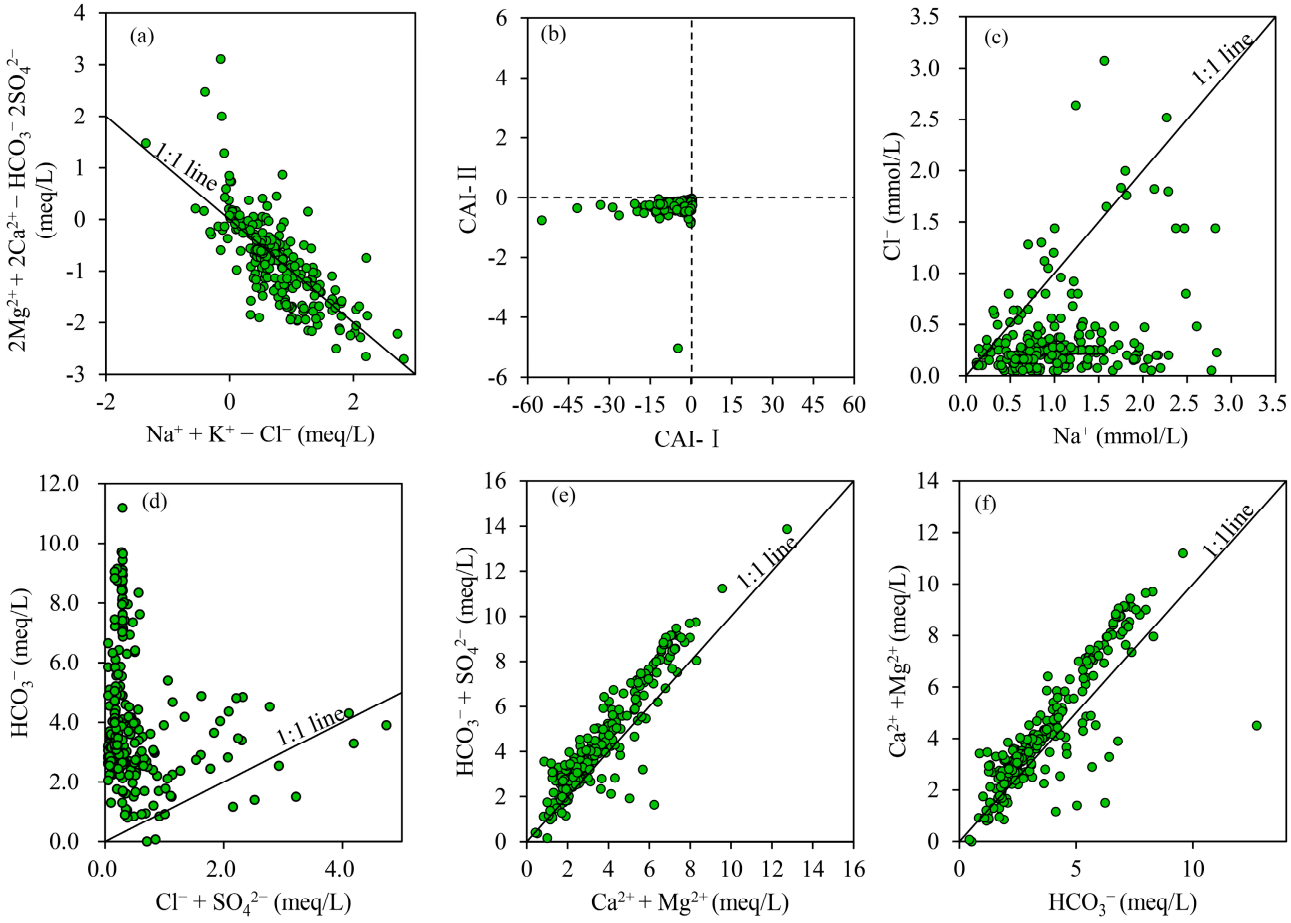

Figure 5. Plots of (**a**) $(Na^+ - Cl^-)$ vs. $[(2SO_4^{2-} + HCO_3^-) - 2(Ca^{2+} + Mg^{2+})]$, (**b**) chlor-alkali indices CAI-Ivs. CAI-II, (**c**) Cl^- vs. Na^+, (**d**) HCO_3^- vs. $Cl^- + SO_4^{2-}$, (**e**) $HCO_3^- + SO_4^{2-}$ vs. $Ca^{2+} + Mg^{2+}$, (**f**) $Ca^{2+} + Mg^{2+}$ vs. HCO_3^-.

The chlor-alkali index (CAI-I and CAI-II) is a water ion exchange test. If CAI-I and CAI-II are negative, then Ca^{2+} and Mg^{2+} exchange with Na^+ and K^+ in groundwater; if CAI-I and CAI-II are positive, then Na^+ and K^+ exchange with Ca^{2+} and Mg^{2+} in groundwater [39,50]. The majority of chlor-alkali indices in groundwater are less than zero, indicating that calcium and magnesium are mostly exchanged for sodium and potassium in groundwater in the research region. It aids in the enrichment of sodium and potassium in groundwater (Figure 5b).

The major source of Na^+ is the dissolution of halite and silicate, and the dissolution of halite results in the same molar concentration of Na^+ and Cl^- [51]. However, the ratio of Na^+ to Cl^- in the water sample is far from the 1:1 line and near that of Na^+ (Figure 4c), showing that the Cl^- content is definitely lower than that of Na^+ and that there should be other anions to balance the excess sodium, indicating that sodium should have other sources. The molar concentration ratio of Na^+/Cl^- ranges from 0.47 to 55.67, with an average of 5.56. This demonstrates that Na^+ is not only derived from the dissolving of rock salt, whereas sodium is mostly derived from the weathering breakdown of silicate rock.

The majority of locations are above and deviate significantly from the $Cl^- + SO_4{}^{2-}$ and $HCO_3{}^-$ 1:1 lines (Figure 5d), indicating that the carbonate source is significantly greater than the evaporate source. The average $(Ca^{2+} + Mg^{2+})/(Na^+ + K^+)$ ratio of groundwater samples in Sanjiang Plain is 3.93, indicating that weathering and carbonate and silicate dissolution are dominant in this region. The correlation coefficient between sodium and calcium is 0.2, suggesting that Na^+ and Ca^{2+} are derived from the same source, implying that some of them are derived via silicate breakdown.

In order to identify whether the hydrochemistry in this region is governed by carbonate rock or gypsum dissolution, $(Ca^{2+} + Mg^{2+})$ and $(HCO_3{}^- + SO_4{}^{2-})$ are usually used to examine the hydrochemical process at the watershed scale [52]. If the equivalent concentration ratio of $(HCO_3{}^- + SO_4{}^{2-})/(Ca^{2+} + Mg^{2+})$ in the water sample is 1:1, carbonate rock or gypsum dissolution controls the hydrochemistry [53,54]. The ratio of $(HCO_3{}^- + SO_4{}^{2-})/(Ca^{2+} + Mg^{2+})$ is greater than 1:1. $(HCO_3{}^- + SO_4{}^{2-})$ exceeds $(Ca^{2+} + Mg^{2+})$ (Figure 5e), indicating that other cations should be present to balance the amount of surplus anions and that there are other sources of $HCO_3{}^-$ in groundwater, some of which originate from silicate dissolution. The correlation coefficients between $HCO_3{}^-$ and Ca^{2+}, Mg^{2+} are 0.806 ($p < 0.01$) and 0.757 ($p < 0.01$), respectively, indicating that they share a common material source, primarily carbonate dissolution. When combined with the Sanjiang Plain's geological history, it suggests that weathering and dissolution of carbonate rocks contribute to Ca^{2+} and $HCO_3{}^-$.

The majority of the points in the figure are in the upper part of the 1:1 ratio (Figure 5f), and the amount of Mg^{2+} and Ca^{2+} is greater than that of $HCO_3{}^-$, with a ratio of around 1.19, indicating that carbonate dissolution cannot explain the composition of Mg^{2+} and Ca^{2+} in groundwater entirely. Cl^- and $SO_4{}^{2-}$ may balance out additional Mg^{2+} and Ca^{2+}. Ca^{2+} and $SO_4{}^{2-}$ have a significant correlation value of 0.251 ($p < 0.01$), indicating that a small amount of halite dissolution is occurring to balance Mg^{2+} and Ca^{2+}.

3.2.2. Human Activity Input

Human actions have a significant impact on the evolution of water chemistry [32,55]. It alters the chemical composition of water by transporting wastewater, waste, and waste gas. $NO_3{}^-$, Cl^-, and $SO_4{}^{2-}$ levels will be higher in areas with high human activity. Of course, weathering can produce Cl^- and $SO_4{}^{2-}$. When water is impacted by human activity, the Cl^-/Na^+ and $NO_3{}^-/Na^+$ ratios are often high. The ratios are rather high (Figure 6), demonstrating that human production and life have an effect on groundwater in this area, which is connected to urban home sewage discharge and large-scale agricultural output.

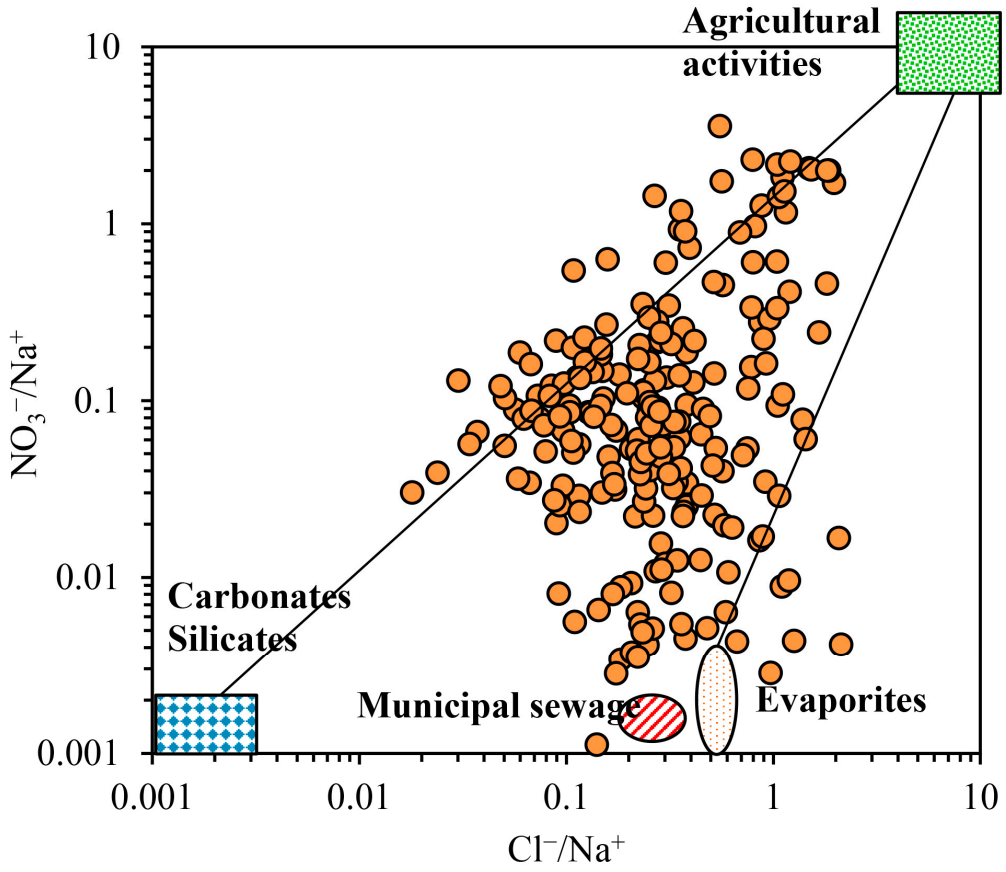

Figure 6. The ratio of Cl^-/Na^+ vs. NO_3^-/Na^+.

3.3. Groundwater Quality

According to the findings of the water quality assessments, the majority of the samples are of high quality (Figure 7a). The EWQI value varied from 2.27 to 91.69, with a mean value of 9.82 obtained from 259 samples. There are 243 high-quality water sources in the research region, accounting for approximately 93.8% of the total. Another nine groundwater samples were categorized as having good water quality, accounting for approximately 3.5% of the total. These two types of water are useful for a variety of applications. Seven samples are rated as medium-grade water, accounting for around 2.7% of the total, which is within the recommended drinking range. There are no samples of water that are of bad or extremely poor quality. The higher the content of NO_3^- in water, the higher the corresponding WQI, indicating that NO_3^- is the main influencing factor of WQI (Figure 7a). The higher the concentration of NO_3^- in water, the higher the corresponding WQI (Figure 7a), indicating that NO_3^- is the primary influencing factor of WQI. The samples with low water quality were primarily dispersed in cities with dense populations, indicating that water quality was directly tied to human activities (Figure 7b).

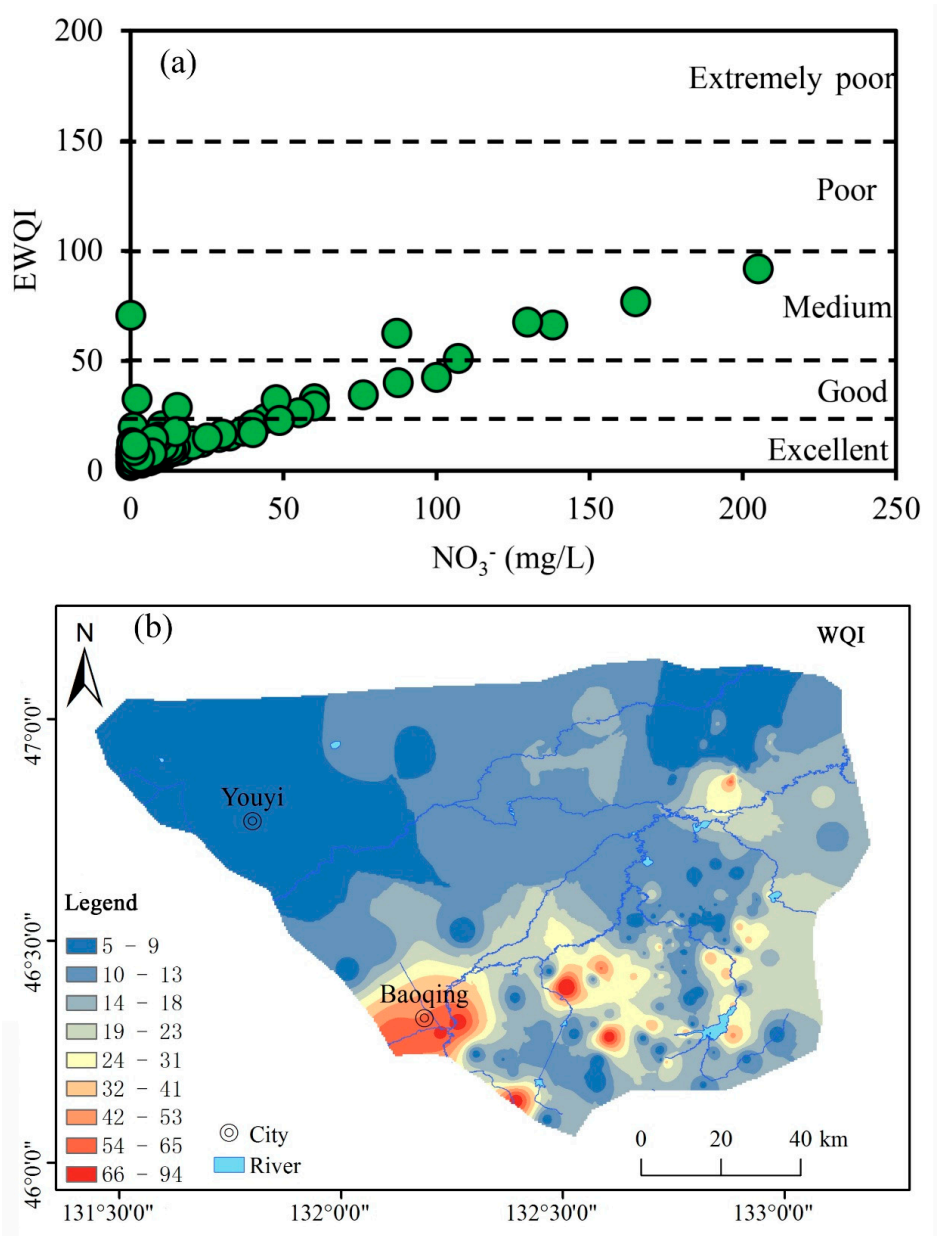

Figure 7. The relationship between WQI and nitrate (**a**) and distribution characteristics of WQI (**b**).

4. Conclusions

Based on the regional scale, this study analyzed the hydrochemical characteristics and hydrochemical evolution of groundwater in Sanjiang Plain, Heilongjiang Province, China and grasped the hydrochemical evolution law of this area. The chemical type of groundwater is Ca-HCO_3, with a cation concentration of $Ca^{2+} > Na^{+} > Mg^{2+} > K^{+}$ and an anion concentration of $HCO_3^{-} > Cl^{-} > SO_4^{2-} > NO_3^{-}$. The chemical composition of water is mainly affected by the dissolution of carbonate rock and silicate rock, and the alternative adsorption of cations and the impact of human activities also play a role. The groundwater quality index results show that the EWQI value is lower than the World Health Organization's drinking water standards, making it suitable for drinking. This study provides a hydrochemical basis for better revealing the interaction mechanism between groundwater and environment and achieving the goal of groundwater management for food security, ecological security, and water supply security in the Sanjiang Plain, and it can serve as a reference for groundwater chemical evolution and water quality evaluation in the global cold area.

Author Contributions: T.Z.: Writing—review and editing; P.W.: Writing—original draft; D.L. and M.W. (Min Wang): Visualization; J.H.: Funding acquisition; M.W. (Mingguo Wang): Funding acquisition: S.X.: Supervision. All authors have read and agreed to the published version of the manuscript.

Funding: This research was funded by China Geological Survey, grant number [DD20230456; DD20230424], and also funded by the National Key R&D Program of China, grant number [2021YFA0715901]. It was also funded by the Medical Education Research Project of Henan Province (Wjlx2020372). And The APC was funded by China Geological Survey.

Data Availability Statement: Not applicable.

Conflicts of Interest: The authors declare that they have no competing interest.

References

1. Döll, P.; Schmied, H.M.; Schuh, C.; Portmann, F.T.; Eicker, A. Global-scale assessment of groundwater depletion and related groundwater abstractions: Combining hydrological modeling with information from well observations and GRACE satellites. *Water Resour. Res.* **2014**, *50*, 5698–5720. [CrossRef]
2. Islam, N.; Irshad, K. Artificial ecosystem optimization with Deep Learning Enabled Water Quality Prediction and Classification model. *Chemosphere* **2022**, *309*, 136615. [CrossRef] [PubMed]
3. Zhang, T.; Cai, W.; Li, Y.; Geng, T.; Zhang, Z.; Lv, Y.; Zhao, M.; Liu, J. Ion chemistry of groundwater and the possible controls within Lhasa River Basin, SW Tibetan Plateau. *Arab. J. Geosci.* **2018**, *11*, 510. [CrossRef]
4. Zhang, H.; Cheng, S.Q.; Li, H.F.; Fu, K.; Xu, Y. Groundwater pollution source identification and apportionment using PMF and PCA-APCA-MLR receptor models in a typical mixed land-use area in Southwestern China. *Sci. Total Environ.* **2020**, *741*, 140383. [CrossRef] [PubMed]
5. Changmai, M.; Pasawan, M.; Purkait, M.K. A hybrid method for the removal of fluoride from drinking water: Parametric study and cost estimation. *Sep. Purif. Technol.* **2018**, *206*, 140–148. [CrossRef]
6. Zhong, C.; Wang, H.; Yang, Q. Hydrochemical interpretation of groundwater in Yinchuan basin using self-organizing maps and hierarchical clustering. *Chemosphere* **2022**, *309*, 136787. [CrossRef]
7. Huang, G.; Song, J.; Han, D.; Liu, R.; Liu, C.; Hou, Q. Assessing natural background levels of geogenic contaminants in groundwater of an urbanized delta through removal of groundwaters impacted by anthropogenic inputs: New insights into driving factors. *Sci. Total Environ.* **2023**, *857*, 159527. [CrossRef]
8. Zhang, Y.; Chen, Z.; Huang, G.; Yang, M. Origins of groundwater nitrate in a typical alluvial-pluvial plain of North China plain: New insights from groundwater age-dating and isotopic fingerprinting. *Environ. Pollut.* **2023**, *316*, 120592. [CrossRef]
9. Du, Y.; Deng, Y.; Ma, T.; Lu, Z.; Shen, S.; Gan, Y.; Wang, Y. Hydrogeochemical evidences for targeting sources of safe groundwater supply in arsenic-affected multi-level aquifer systems. *Sci. Total Environ.* **2018**, *645*, 1159–1171. [CrossRef]
10. Smith, R.G.; Majumdar, S. Groundwater storage loss associated with land subsidence in western United States mapped using machine learning. *Water Resour. Res.* **2020**, *56*, e2019WR026621. [CrossRef]
11. Harkness, J.S.; Jurgens, B.C. Effects of imported recharge on fluoride trends in groundwater used for public supply in California. *Sci. Total Environ.* **2022**, *830*, 154782. [CrossRef]
12. Gill, B.; Webb, J.; Stott, K.; Cheng, X.; Wilkinson, R.; Cossens, B. Economic, social and resource management factors influencing groundwater trade: Evidence from Victoria, Australia. *J. Hydrol.* **2017**, *550*, 253–267. [CrossRef]
13. Chen, R.H.; Tenga, Y.G.; Chen, H.Y.; Hu, B.; Yue, W.F. Groundwater pollution and risk assessment based on source apportionment in a typical cold agricultural region in Northeastern China. *Sci. Total Environ.* **2019**, *696*, 133972. [CrossRef] [PubMed]
14. Yang, Q.; Li, Z.; Ma, H.; Wang, L.; Martín, J.D. Identification of the hydrogeochemical processes and assessment of groundwater quality using classic integrated geochemical methods in the Southeastern part of Ordos basin, China. *Environ. Pollut.* **2016**, *218*, 879–888. [CrossRef] [PubMed]
15. Emenike, P.C.; Tenebe, I.T.; Neris, J.B.; Omole, D.O.; Afolayan, O.; Okeke, C.U.; Emenike, I.K. An integrated assessment of land-use change impact, seasonal variation of pollution indices and human health risk of selected toxic elements in sediments of River Atuwara, Nigeria. *Environ. Pollut.* **2020**, *265*, 114795. [CrossRef]
16. Goswami, R.; Neog, N.; Bhagat, C.; Hdeib, R.; Mahlknecht, J.; Kumar, M. Arsenic in the groundwater of the Upper Brahmaputra floodplain: Variability, health risks and potential impacts. *Chemosphere* **2022**, *306*, 135621. [CrossRef]
17. Devaraj, N.; Panda, B.; Chidambaram, S.; Prasanna, M.V.; Singh, D.K.; Ramanathan, A.L.R.; Sahoo, S.K. Spatio-temporal variations of uranium in groundwater: Implication to the environment and human health. *Sci. Total Environ.* **2021**, *775*, 145787.
18. Li, X.; Huang, X.; Zhang, Y. Spatio-temporal analysis of groundwater chemistry, quality and potential human health risks in the Pinggu basin of North China Plain: Evidence from high-resolution monitoring dataset of 2015–2017. *Sci. Total Environ.* **2021**, *800*, 149568. [CrossRef]
19. Elumalai, V.; Rajmohan, N.; Sithole, B.; Li, P.; Uthandi, S.; Tol, J. Geochemical evolution and the processes controlling groundwater chemistry using ionic ratios, geochemical modelling and chemometric analysis in uMhlathuze catchment, KwaZulu-Natal, South Africa. *Chemosphere* **2022**, *312*, 137179. [CrossRef]

20. Lin, L.; Zhang, Y.; Qian, X.; Wang, Y. Hydrochemical Characteristics and Human Health Risk Assessment of Surface Water in the Danjiang River Source Basin of the Middle Route of China's South-to-North Water Transfer Project. *Water* **2023**, *15*, 2203. [CrossRef]
21. Wu, J.J.; Bian, J.M.; Wan, H.L.; Ma, Y.X.; Sun, X.Q. Health risk assessment of groundwater nitrogen pollution in Songnen Plain. *Ecotoxicol. Environ. Saf.* **2021**, *207*, 111245. [CrossRef] [PubMed]
22. Zhao, C.; Zhang, X.G.; Fang, X.; Zhang, N.; Xu, X.Q.; Li, L.H.; Liu, Y.; Su, X.; Xia, Y. Characterization of drinking groundwater quality in rural areas of Inner Mongolia and assessment of human health risks. *Ecotoxicol. Environ. Saf.* **2022**, *234*, 113360. [CrossRef] [PubMed]
23. Jia, Z.; Bian, J.M.; Wang, Y. Impacts of urban land use on the spatial distribution of groundwater pollution, Harbin City, Northeast China. *J. Contam. Hydrol.* **2018**, *215*, 29–38. [CrossRef] [PubMed]
24. Zhao, G.; Li, W.; Li, F.; Zhang, F.; Liu, G.C. Hydrochemistry of waters in snowpacks, lakes and streams of Mt. Dagu, eastern of Tibet Plateau. *Sci. Total Environ.* **2018**, *610–611*, 641–650. [CrossRef]
25. Li, Q.; Zhao, D.; Yin, J.; Zhou, X.; Li, Y.; Chi, P.; Han, Y.; Ansari, U.; Cheng, Y. Sediment Instability Caused by Gas Production from Hydrate-bearing Sediment in Northern South China Sea by Horizontal Wellbore: Evolution and Mechanism. *Nat. Resour. Res.* **2023**, *32*, 1595–1620. [CrossRef]
26. Wang, F.; Liu, X.; Jiang, B.; Zhuo, H.; Chen, W.; Chen, Y.; Li, X. Low-loading Pt nanoparticles combined with the atomically dispersed FeN4 sites supported by FeSA-N-C for improved activity and stability towards oxygen reduction reaction/hydrogen evolution reaction in acid and alkaline media. *J. Colloid Interface Sci.* **2023**, *635*, 514–523. [CrossRef]
27. Li, Q.; Zhang, C.; Yang, Y.; Ansari, U.; Han, Y.; Li, X.; Cheng, Y. Preliminary experimental investigation on long-term fracture conductivity for evaluating the feasibility and efficiency of fracturing operation in offshore hydrate-bearing sediments. *Ocean Eng.* **2023**, *281*, 114949. [CrossRef]
28. Nixdorf, E.; Sun, Y.Y.; Lin, M.; Kolditz, O. Development and application of a novel method for regional assessment of groundwater contamination risk in the Songhua River Basin. *Sci. Total Environ.* **2017**, *605–606*, 598–609. [CrossRef]
29. Zhang, B.; Song, X.F.; Zhang, Y.H.; Han, D.M.; Tang, C.Y.; Yang, L.H.; Wang, Z.L. The renewability and quality of shallow groundwater in Sanjiang and Songnen Plain, Northeast China. *J. Integr. Agric.* **2017**, *16*, 229–238. [CrossRef]
30. Liu, Y.L.; Jin, M.G.; Wang, J.J. Insights into groundwater salinization from hydrogeochemical and isotopic evidence in an arid inland basin. *Hydrol. Process.* **2018**, *32*, 3108–3127. [CrossRef]
31. *GB/T 5750*; Standards for Drinking Water Quality. Ministry of Health of the People's Republic of China: Beijing, China, 2006.
32. *DZ/T 0064*; MAGQ, Methods for Analysis of Groundwater Quality. Ministry of Natural Resources of the People's Republic of China: Beijing, China, 2021.
33. Paca, J.M.; Santos, F.M.; Pires, J.C.M.; Leitão, A.A.; Boaventura, R.A.R. Quality assessment of water intended for human consumption from Kwanza, Dande and Bengo rivers (Angola). *Environ. Pollut.* **2019**, *254*, 113037. [CrossRef] [PubMed]
34. Adimalla, N. Application of the entropy weighted water quality index (EWQI) and the pollution index of groundwater (PIG) to assess groundwater quality for drinking purposes: A case study in a rural area of Telangana State, India. *Arch. Environ. Contam. Toxicol.* **2021**, *80*, 31–40. [CrossRef] [PubMed]
35. Liu, J.T.; Gao, Z.J.; Zhang, Y.Q.; Sun, Z.B.; Sun, T.Z.; Fan, H.B.; Wu, B.; Li, M.B.; Qian, L.L. Hydrochemical evaluation of groundwater quality and human health risk assessment of nitrate in the largest peninsula of China based on high-density sampling: A case study of Weifang. *J. Clean. Prod.* **2021**, *322*, 129164. [CrossRef]
36. *GB/T 14848-2017*; Standards for Groundwater Quality. National Standard of People's Republic of China: Beijing, China, 2017.
37. Chai, N.; Yi, X.; Xiao, J.; Liu, T.; Liu, Y.; Deng, L.; Jin, Z. Spatiotemporal variations, sources, water quality and health risk assessment of trace elements in the Fen River. *Sci. Total Environ.* **2021**, *757*, 143882. [CrossRef]
38. Gibbs, R.J. Mechanisms controlling world water chemistry. *Science* **1970**, *170*, 1088–1090. [CrossRef] [PubMed]
39. Zhang, Y.; Dai, Y.; Wang, Y.; Huang, X.; Xiao, Y.; Pei, Q. Hydrochemistry, quality and potential health risk appraisal of nitrate enriched groundwater in the Nanchong area, southwestern China. *Sci. Total Environ.* **2021**, *784*, 147186. [CrossRef]
40. Ke, X.; Li, Y.; Wang, W.; Niu, F.; Gao, Z. Hydrogeochemical characteristics and processes of thermokarst lake and groundwater during the melting of the active layer in a permafrost region of the Qinghai-Tibet Plateau, China. *Sci. Total Environ.* **2022**, *851*, 158183. [CrossRef]
41. Wang, Y.; Li, P. Appraisal of shallow groundwater quality with human health risk assessment in different seasons in rural areas of the Guanzhong Plain (China). *Environ. Res.* **2022**, *207*, 112210. [CrossRef]
42. Xiao, J.; Lv, G.R.; Chai, N.P.; Hu, J.; Jin, Z.D. Hydrochemistry and source apportionment of boron, sulfate, and nitrate in the Fen River, a typical loess covered area in the eastern Chinese Loess Plateau. *Environ. Res.* **2022**, *206*, 112570. [CrossRef]
43. Gao, Y.Y.; Qian, H.; Zhou, Y.H.; Chen, J.; Wang, H.K.; Ren, W.H.; Qu, W.G. Cumulative health risk assessment of multiple chemicals in groundwater based on deterministic and Monte Carlo models in a large semiarid basin. *J. Clean. Prod.* **2022**, *352*, 131567. [CrossRef]
44. Sunkari, E.D.; Seidu, J.; Ewusi, A. Hydrogeochemical evolution and assessment of groundwater quality in the Togo and Dahomeyan aquifers, Greater Accra Region, Ghana. *Environ. Res.* **2022**, *208*, 112679. [CrossRef] [PubMed]
45. Wang, M.; Wang, M.; Yang, L.; Yang, T.; Li, J.; Chen, Y. Distribution Characteristics and Genesis of Iron and Mangnese Ions in Groundwater of Eastern Sanjiang Plain, China. *Water* **2023**, *15*, 2068. [CrossRef]

46. Gaillardet, J.; Dupre, B.; Louvat, P.; Allegre, C.J. Global silicate weathering and CO_2 consumption rates deduced from the chemistry of large rivers. *Chem. Geol.* **1999**, *159*, 3–30. [CrossRef]
47. Shen, B.B.; Wu, J.L.; Zhan, S.E.; Jin, M.; Saparov, A.S.; Abuduwaili, J. Spatial variations and controls on the hydrochemistry of surface waters across the Ili-Balkhash Basin, arid Central Asia. *J. Hydrol.* **2021**, *600*, 126565. [CrossRef]
48. Zhang, X.; Miao, J.; Hu, B.X.; Liu, H.; Zhang, H.; Ma, Z. Hydrogeochemical characterization and groundwater quality assessment in intruded coastal brine aquifers (Laizhou Bay, China). *Environ. Sci. Pollut. Res.* **2017**, *24*, 21073–21090. [CrossRef] [PubMed]
49. Argamasilla, M.; Barbera, J.A.; Andreo, B. Factors controlling groundwater salinization and hydrogeochemical processes in coastal aquifers from southern Spain. *Sci. Total Environ.* **2017**, *580*, 50–68. [CrossRef]
50. Ha, Q.K.; Ngoc, T.D.T.; Vo, P.L.; Nguyen, H.Q.; Dang, D.H. Groundwater in Southern Vietnam: Understanding geochemical processes to better preserve the critical water resource. *Sci. Total Environ.* **2022**, *807*, 151345. [CrossRef]
51. Borrok, D.M.; Lenz, R.M.; Jennings, J.E.; Gentry, M.L.; Steensma, J.; Vinson, D.S. Applied Geochemistry the origins of high concentrations of iron, sodium, bicarbonate, and arsenic in the Lower Mississippi River Alluvial Aquifer. *Appl. Geochem.* **2018**, *98*, 383–392. [CrossRef]
52. Wang, H.L.; Hussaini, K.M.; Zhang, H.; Rinklebe, J. Hydrogeochemical and health risk evaluation of arsenic in shallow and deep aquifers along the different floodplains of Punjab, Pakistan. *J. Hazard. Mater.* **2021**, *402*, 124074.
53. Brindha, K.; Paul, R.; Walter, J.; Tan, M.L.; Singh, M.K. Trace metals contamination in groundwater and implications on human health: Comprehensive assessment using hydrogeochemical and geostatistical methods. *Environ. Geochem. Health* **2020**, *42*, 3819–3839. [CrossRef]
54. Wang, Z.Y.; Su, Q.; Wang, S.; Gao, Z.J.; Liu, J.T. Spatial distribution and health risk assessment of dissolved heavy metals in groundwater of eastern China coastal zone. *Environ. Pollut.* **2021**, *290*, 118016. [CrossRef] [PubMed]
55. Adimalla, N.; Qian, H. Groundwater chemistry, distribution and potential health risk appraisal of nitrate enriched groundwater: A case study from the semi-urban region of South India. *Ecotoxicol. Environ. Saf.* **2021**, *207*, 111277. [CrossRef] [PubMed]